Accepted Manuscript

Title: An electrochemical DNA-sensor developed with the use of Methylene Blue as a redox indicator for the detection of DNA damage induced by endocrine-disrupting compounds

Author: Xiaoyun Lin Yongnian Ni Serge Kokot

PII: S0003-2670(15)00228-7
DOI: http://dx.doi.org/doi:10.1016/j.aca.2015.02.050
Reference: ACA 233764

To appear in: *Analytica Chimica Acta*

Received date: 18-11-2014
Revised date: 13-2-2015
Accepted date: 18-2-2015

Please cite this article as: Xiaoyun Lin, Yongnian Ni, Serge Kokot, An electrochemical DNA-sensor developed with the use of Methylene Blue as a redox indicator for the detection of DNA damage induced by endocrine-disrupting compounds, Analytica Chimica Acta http://dx.doi.org/10.1016/j.aca.2015.02.050

An electrochemical DNA-sensor developed with the use of Methylene Blue as a redox indicator for the detection of DNA damage induced by endocrine-disrupting compounds

Xiaoyun Lin [a,b], Yongnian Ni [a,b]*, Serge Kokot [c]

[a] *State Key Laboratory of Food Science and Technology, Nanchang University, Nanchang 330047, China*

[b] *College of Chemistry, Nanchang University, Nanchang 330031, China*

[c] *School of Chemistry, Physics and Mechanical Engineering, Queensland University of Technology, Brisbane 4001, Australia*

* Corresponding author. Address: Department of Chemistry, Nanchang University, Nanchang 330031, China. Tel./Fax: 86 791 83969500. E-mail address: ynni@ncu.edu.cn (Y. Ni), s.kokot@qut.edu.au (S. Kokot)

Graphic Abstract

An electrochemical DNA-sensor developed with the use of Methylene Blue as a redox indicator for the detection of DNA damage induced by endocrine-disrupting compounds

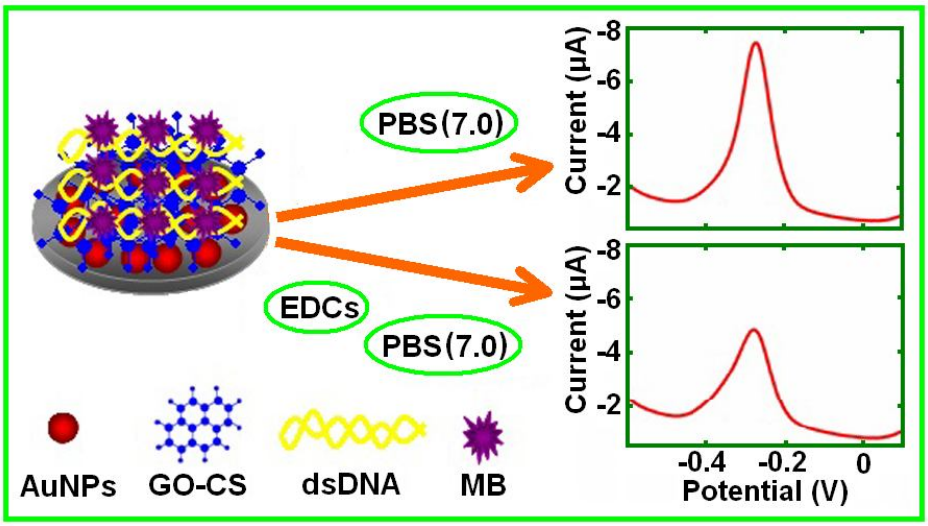

Highlights

► A new method for detecting DNA damage was successfully developed
► A novel biosensor, MB/dsDNA/GO-CS/AuNPs/GCE biosensor was constructed
► Loading/release of MB in/out of dsDNA/GO-CS/AuNPs film was investigated
► DNA damage induced by BPA, NP and OP was detected and estimated

Abstract

An electrochemical biosensor capable of indirect detection of DNA damage induced by any one of the three endocrine-disrupting compounds (EDCs) - bisphenol A (BPA), 4-nonylphenol (NP) and 4-t-octylphenol (OP), has been researched and developed. The Methylene Blue (MB) dye was used as the redox indicator. The glassy carbon electrode (GCE) was modified by the assembled dsDNA/graphene oxide-chitosan/gold nano–particles to produce a dsDNA/GO-CS/AuNPs/GCE sensor. It was characterized with the use of electrochemical impedance spectroscopy (EIS), cyclic voltammetry (CV) and scanning electron microscopy (SEM) techniques. The loading/release of the MB dye by the dsDNA/GO-CS/AuNPs film was investigated, and the results showed that the process was reversible. Based on this, the sensor was used to measure the difference between the loading capabilities of intact and damaged dsDNA in the films. The sensor was then successfully applied to detect DNA damage electrochemically. The differential pulse voltammetry (DPV) peak current ratio for MB, observed before and after DNA damage, increased linearly in the presence the BPA, NP or OP compounds; the treatment range was 10 to 60 min, and the respective damage rates were 0.0069, 0.0044 and 0.0031 min^{-1}, respectively. These results were confirmed by the binding constants: 2.09×10^{6} M^{-1} (BPA-DNA), 1.28×10^{6} M^{-1} (NP-DNA) and 9.33×10^{5} M^{-1} (OP-DNA), all of which were obtained with the use of differential pulse stripping voltammetry (DPSV).

Keywords: DNA–damage; Electrochemical DNA–sensor; Methylene Blue dye; Endocrine–disrupting chemicals.

1. Introduction

Deoxyribonucleic acid (DNA) encodes the genetic instructions used in the development and functioning of all known living organisms and many viruses [1]. DNA together with proteins and carbohydrates , belongs to a group of major macromolecules, which are essential for all known forms of life [2].

The phrase, 'DNA damage', refers to a DNA molecule, whose chemical structure has been altered by chemical and/or physical means. Examples of physical factors include high temperature [3], ultraviolet radiation [4] and other ionizing radiation [5]. There are numerous chemical factors, which can lead to DNA damage, and among others, they include reactions with O_2, H_2O_2 and other chemicals involved with the biological metabolism, as well as various types of free radicals generated spontaneously or induced in an organism. Additionally, approximately 10 million tons of toxic chemicals are released annually into the environment by industrial sources [6]. Many of these chemicals, such as heavy metal ions, vinyl chloride, polycyclic aromatic hydrocarbons, pesticides and their metabolites, are geno-toxic and form covalent adducts with DNA, leading to mutagenesis and carcinogenesis [7–10]. Therefore, rapid, inexpensive and sensitive methods of analysis of DNA damage are important, and similarly, screening of new medicines *in vitro* for potential gene toxicity is essential, before their commercial use [11,12].

Various analytical methods have been reported for the detection of DNA damage. These include electrophoresis [13,14] and spectroscopic methods [15] as well as the DNA chip, molecular probe technologies [16] and electrochemical methods [10,17–20]. The electrochemical methods are of particular interest because they are uncomplicated, have rapid responses, relatively cheap to run and, generally, analytically, quite sensitive. The electrochemical detection of DNA damage commonly requires the immobilization of the DNA on the surface of an electrode. This has been achieved with the use of different methods such as adsorption, casting, covalent attachment and layer–by–layer assembly. The last mentioned approach requires the deposition of alternating layers of oppositely charged materials on solid surfaces by electrostatic interaction [11,18].

Endocrine-disrupting compounds (EDCs) are substances that can interfere with the normal, hormonal function of humans or animals, and thus, pose a potential threat to the environment and human health [21]. Such compounds are therefore, of global interest. Bisphenol A (BPA), 4-t-octylphenol (OP) and

4-nonylphenol (NP) (Scheme 1) are synthesised alkylphenols, which are such successful endocrine disruptors that they are produced and used on a wide scale [22].

BPA is a compound, which is extensively used in industry as an important intermediate in the production of resins and polymers such as poly–carbonate, –sulphone, –acrylate as well as epoxies, unsaturated polyesters and phenolics [23]. Additionally, BPA can also be found in common products such as bottles, food packaging, nail polishes, and flame-retardant materials amongst many others. Recently, European Union (E.U.), in a landmark decision, has banned the use of BPA in plastic feeding or drinking bottles for infants [24]. The other two compounds, OP and NP, are common additives, which are found, for example, in lubricating oils, paints, and cosmetics amongst other products [25,26].

Gold nanoparticles (AuNPs) have been used to build biosensors because of their unique optical, electronic, and catalytic properties [27,28]. Also, the AuNPs provide an environment similar to that in nature such that the bioactivity of an immobilized biomolecule is maintained; additionally, the nanoparticles provide a relatively high surface area–to–volume ratio and enhance the electron transfer kinetics [29].

Graphene oxide (GO) consists of a single, polymerized layer of carbon atoms closely packed into a two–dimensional honeycomb lattice [30,31]; such GO films in sensors are known to be effective sensing platforms for small molecules.

In this work, 3,7-bis(dimethylamino)phenothiazin-5-ium chloride (Methylene Blue, MB) was used as the redox active molecule to detect the DNA damage. MB is a derivative of anthraquinone, and can intercalate into the double helix structure of dsDNA. Hu et al. [32] developed an electrochemical sensor for the detection of damage on natural dsDNA. This was induced by styrene oxide adsorbed on PSS/(PDDA/dsDNA)$_3$ layer–by–layer films and using MB as an electroactive probe.

Chitosan (CS) is a kind of natural polysaccharide, and has an isoelectric point value of 6; it is positively charged at pH 5.5, while DNA has many negative charges on its sugar-phosphate backbone. Thus, in the present work, oppositely charged CS at pH 5.5 and DNA were assembled into GO-CS/DNA films on solid surfaces and were stabilised mainly by coulombic attraction [9].

Many studies [33-36] have shown that BPA, OP and NP can form covalent adducts with DNA. Compared with the intact DNA films, the BPA, OP or NP – damaged DNA films exhibited a significant decrease in DPV peak currents for MB. Thus, the extent of DNA damage could be estimated according to the size of

these decreased currents. Additionally, the binding constants of the species formed between the EDCs and DNA can be extracted with the use of differential pulse stripping voltammetry (DPSV), and these constants can be used to support or otherwise the presence of DNA damage.

2. Experimental

2.1. Reagents

The following chemical reagents were purchased: Hydrogen tetrachloroaurate tetrahydrate ($HAuCl_4 \cdot 4H_2O$), dsDNA and chitosan (Aldrich Co., U.S.); BPA, NP and OP (Aladdin Chemistry Co., Ltd, Shanghai, China); Graphene Oxide (GO) (Chengdu Organic Chemicals Co. Ltd., Chinese Academy of Sciences, Chengdu, China). All other chemicals (Analytical Grade reagents) were obtained from Beijing Chemical Reagent Company (Beijing, China) and used without further purification. Phosphate buffer solution (PBS, 0.05 M, pH 7.00) was the supporting electrolyte, and was prepared from KH_2PO_4 and K_2HPO_4 salts; the buffer pH was monitored with an Orion SA720 meter (U.S.). Double–distilled water was used throughout the experiments.

2.2. Instrumentation

Electrochemical experiments were performed with the use of a CHI660A electrochemical workstation (Chenhua Apparatus Co., Shanghai, China) in conjunction with a three–electrode system: the working electrode – dsDNA/GO-CS/AuNPs/GCE (3 mm diameter), the counter electrode – a platinum wire, and the reference – a saturated calomel electrode (SCE). Electrode potentials were reported with respect to the SCE. A cell stand (Model BAS C1A) was used for voltammetric scanning and to stir the testing solution during the pre-concentration step.

Scanning electron microscopy (SEM) images were obtained using a Quanta200F instrument (FEI Ltd, Tokyo, Japan). The samples were electro–deposited or dropped onto the detachable GCE. The power level was 20 kV.

2.3. Preparation of the dsDNA/GO–CS/AuNPs/GCE

Glassy carbon electrodes (GCE, 3 mm diameter) were polished with emery paper and alumina slurry. They

were then rinsed thoroughly with dilute nitric acid, ethanol, and distilled water in an ultrasonic bath; then, they were electrochemically subjected to potential cycling between −1.0 and 1.0 V in 0.25 mol L^{-1} H_2SO_4 until a steady state was reached. Finally, the clean GCE was immersed into 1.0×10^{-3} mol L^{-1} $HAuCl_4$ containing 0.01 mol L^{-1} Na_2SO_4 and 0.01 mol L^{-1} H_2SO_4, and the gold nanoparticles were electrodeposited at −0.2 V (*versus*. SCE) for 30 s. The results showed that the particle distribution after 30 s deposition time was apparently quite uniform, and the particles were also homogeneous [37]. Finally, the completed electrode (AuNPs/GCE) was rinsed with twice-distilled water.

Stock solution of chitosan (CS) (0.5 wt%) was prepared in 0.1 mol L^{-1} acetic acid. Any undissolved materials were filtered (Whatman filter paper (11 μm), Voigt Global Distribution Inc. Lawrence, Kansas, U.S.), and solution pH was adjusted to 5.5 with the addition of 0.5 mol L^{-1} NaOH and vigorous stirring. 1.0 mg GO was added to 1.0 mL of the 0.5 wt% chitosan solution, followed by ultra−sonication for 2 h to form a homogenous mixture of GO–CS. Subsequently, 15 μL of this mixture was then deposited dropwise on the surface of the AuNPs/GCE. The solvent was then allowed to evaporate in air for 3 h, and then the electrode surface was thoroughly rinsed with redistilled, deionized water and dried in air [38].

DNA solution (1.0 mg mL^{-1}) was prepared by dissolving 50.0 mg of solid dsDNA in 50 mL 50 mmol L^{-1} sodium chloride solution. Subsequently, 20 μL 1.0 mg mL^{-1} dsDNA stock solution was deposited on the surface of the GO-CS/AuNPs/GCE and dried for 5 h in air at room temperature. The obtained dsDNA/GO-CS/AuNPs/GCE was washed with deionized water and immersed in PBS (pH 7.00) for 5 min to remove any loosely adsorbed DNA.

2.4. Experimental

2.4.1. Loading/release/reloading of MB in the DNA/GO-CS/AuNPs film

MB–loaded dsDNA/GO-CS/AuNPs films were made by immersing the dsDNA/GO-CS/AuNPs coated electrodes in MB (1mmol L^{-1}) dissolved in PBS buffer solutions (pH 7.0) for a preselected period of time; such films were referred to as MB-dsDNA/GO-CS/AuNPs. The electrodes with the loaded films were then rinsed thoroughly in twice–distilled water, dried in a stream of dry nitrogen gas, and then placed in PBS (pH 7.0) for DPV scans. At this point of preparation, the condition of the MB-dsDNA/GO-CS/AuNPs film was defined to be in State I (Scheme 2), and the corresponding DPV peak current as $I_{P,I}$. The film was then kept in

the PBS at 25 ± 0.5 °C with stirring, for over 4 h so as to extract most of the MB, which was not specifically bound. The DPV scans were collected with the electrodes immersed in the same PBS. At this stage of preparation, the condition of the MB-dsDNA/GO-CS/AuNPs film was defined to be in State II (Scheme 2) and the corresponding DPV peak current was $I_{P,II}$.`

For the DNA damage experiments, the MB-dsDNA/GO-CS/AuNPs film in State II was treated in 1.0×10^{-5} mol L^{-1} BPA, NP or OP solution, with stirring, for a given time at 37 °C, respectively. After this treatment, the damaged film electrodes were rinsed with twice–distilled water, dried in a stream of nitrogen, and immersed in PBS (pH 7.0) in readiness for collection of the DPV scans. At this stage of preparation, the MB-dsDNA/GO-CS/AuNPs film was defined to be in State III (Scheme 2), and the corresponding DPV peak current was labeled, $I_{P,III}$.

The above treated electrode (State III) was soaked in the MB (1.0 mmol L^{-1}) / PBS (pH 7.0) solution for at least 2 h so as to reload MB, and then this electrode was immersed in the PBS for DPV scanning. The MB-dsDNA/GO-CS/AuNPs film, at this stage damaged by BPA, NP or OP, was defined to be in State IV (Scheme 2), and the corresponding DPV peak current was labelled $I_{P,IV}$. Each treatment and the associated measurements were repeated at least three times.

2.4.2. Interaction of BPA, NP or OP with dsDNA

For the DPSV experiments, the concentrations of BPA, NP or OP were kept at 2.5×10^{-6} mol L^{-1}, and the DNA was added at different concentrations in the range of 0.0 to 4.0×10^{-6} mol L^{-1} at intervals of 5.0×10^{-7} mol L^{-1} (total: nine analytical samples). The potential was scanned from 0.2 to 1.0 V with a scan rate of 100 mV s^{-1}, pulse width of 50 ms, pulse amplitude of 25 mV, and deposition time of 60 s. All experiments were carried out in PBS (pH 7.0) at 25 ± 1 °C.

3. Results and discussion

3.1. Characterization of dsDNA/GO-CS/AuNPs/GCE

Scanning electron microscopy (SEM) images (Fig. 1) showed various aspects of morphology of the untreated GCE (**A**), AuNPs/GCE (**B**) and GO-CS/AuNPs/GCE (**C**). The surface of the untreated GCE appeared to be relatively smooth (Fig. 1A) but after the electro-deposition of the gold nanoparticles for 30s, it was more or less covered by globular nanoparticles with diameters of approximately 100–150 nm, (Fig. 1B). When

GO–CS was deposited on the AuNPs/GCE, a very uneven, crumpled, and layered structure of the graphene film seemed to form on the surface of the GCE (Fig. 1C).

The electrochemical properties of the modified electrodes were investigated with the use of the electrochemical impedance spectroscopy (EIS) and cyclic voltammetry (CV) (Fig. 2), and the experiments were performed in 5×10^{-3} mol L^{-1} $[Fe(CN)_6]^{3-/4-}$ (1:1) solution containing 0.1 mol L^{-1} KCl.

In general, typical EIS data consists of the electron–transfer resistance (R_{et}) values at the electrode's surface, and when presented on a Nyquist plot, such data is often distributed as a semi–circle, the diameter of which is related to the properties at the interface of the electrode [39]. Such plots display changes of the semicircular diameters (R_{et}) in the Z' (the real part of the impedance) *versus* Z" (the imaginary part) space, i.e. the Nyquist plots. In this work, the changes in such plots were investigated as a function of the modification of the film on the working electrode, i.e from its GCE state to the fully modified dsDNA/GO-CS/AuNPs/GCE (Fig. 2A). In this context, for the untreated GCE, a small well–defined semi–circle (R_{et}) was obtained at higher frequencies (a in Fig. 2A); this indicated the presence of a small impedance at the interface. When the AuNPs were electro-deposited on the surface of the GCE, these impedance values (R_{et}) were further reduced as compared to those from the GCE. This indicated that the AuNPs/GCE (b in Fig. 2A) was strongly conducting. When GO-CS was introduced onto the AuNPs/GCE surface (c in Fig. 2A), the impedance values (R_{et}) did not show any significant changes compared with that from the AuNPs/GCE, and this indicated an even smaller interface electron transfer resistance. This could occur because CS is positively charged at pH 5.5. Given this, the electrostatic attraction between $[Fe(CN)_6]^{3-/4-}$ and the positively charged sensing platform facilitated the diffusion of $[Fe(CN)_6]^{3-/4-}$ to the electrode's surface [40]. However, when the fully modified dsDNA/GO-CS/AuNPs/GCE (d in Fig. 2A) was tested, the impedance curve of the modified electrode included a relatively well formed semicircle. This indicated a relatively high electron transfer resistance and suggested that the DNA was immobilized on the GO-CS/AuNPs film.

CV experiments with the same electrode systems and in the presence of the same redox probe, $[Fe(CN)_6]^{3-/4-}$, produced results (Fig. 2B), which supported the conclusions obtained from the EIS work. Thus, at the untreated GCE electrode, CV oxidation and reduction profiles were observed as expected (a in Fig. 2B); profiles b and c (Fig. 2B) were expected to show more intense CV responses because AuNPs with their good

electrical conductivity, and CS with its positive charge, should have facilitated the electron transfer to the electrode's surface. When DNA was deposited on the surface of the GO-CS/AuNPs/GCE (d in Fig. 2B), the current response of $[Fe(CN)_6]^{3-/4-}$ decreased, again as expected, leading to the least intense profiles. This observation is most likely to be related to the electrostatic repulsion between the poly-anionic DNA on the modified electrode and the anionic redox ions in the solution. In general, the CV results supported those from the EIS (Fig. 2A).

Chronocoulometric curves of the reduction of $K_3[Fe(CN)_6]$ (5×10^{-3} mol L^{-1}) in KCl (0.1 mol L^{-1}) obtained from different electrodes were used to compare the apparent electrode areas. According to Equation 1 [41]:

$$Q = (2nFAD_0^{1/2}\pi^{-1/2}C_0)\, t^{1/2} \quad (1)$$

where: Q − absolute reduction charge, n − number of electrons transferred, F − Faraday constant, A − apparent electrode area, t − time, D_0 − diffusion coefficient and C_0 − bulk concentration of the oxidized form of the hexacyanoferrate (III) complex. The electrode area, A, may be estimated from the slope of the Q versus $t^{1/2}$ plot (Fig. 2C). Thus, the order of the slope values was: GO-CS/AuNPs/GCE (a) > CS/AuNPs/GCE (b) > AuNPs/GCE (c) > GCE (d), i.e. GO-CS/AuNPs/GCE has the largest A value.

3.2. Influence of the differently modified electrodes on the MB loading

Each of the five electrodes, dsDNA/GCE, dsDNA/AuNPs/GCE, dsDNA/CS/AuNPs/GCE, dsDNA/GO-CS /AuNPs/GCE and GO-CS/AuNPs/GCE was immersed separately in MB (1mmol L^{-1}) PBS (pH 7.0) for 2 h, and the modified electrodes were then rinsed with doubly-distilled water, dried in a stream of nitrogen and immersed in PBS (pH 7.0) for DPV scans. Compared with the MB-dsDNA/GCE (a in Fig. 3), and the other two modified electrodes (b and c in Fig. 3), the MB-dsDNA/GO-CS/AuNPs/GCE (d in Fig. 3) produced the most intense DPV peak current. This showed that the dsDNA/GO-CS/AuNPs/GCE had the relatively highest MB loading of the four types of electrode (a − d) investigated. However, compared with the other four electrodes (a, b, c and d in Fig. 3), the oxidation peak potential of the MB-GO-CS/AuNPs/GCE (e in Fig. 3) shifted to about 36 mV in the negative direction, and its oxidation peak current was considerably lower than that of the MB-dsDNA /GO-CS/AuNPs/GCE. The results showed that MB interacted mainly with the dsDNA, and not the GO-CS system.

This observation can be explained by noting that the GO-CS/AuNPs/GCE has a large surface area, and thus,

can absorb many DNA molecules. Also, it has been demonstrated [42] that there are two modes of interaction between MB and DNA – one depends on strong binding and involves semi−intercalation, and the other involves relatively weak binding via electrostatic interactions. Consequently, the DNA/GO-CS/AuNPs/GCE can interact with many MB molecules. Thus, all of these observations showed that the GO–CS was an effective sensing platform for the immobilization of DNA.

3.3. Loading/releasing of MB at the dsDNA/GO-CS/AuNPs film

In order to investigate the reversibility of the loading/releasing behavior of MB onto and from the film, the fully loaded MB-dsDNA/GO-CS/AuNPs/GCE was immersed in PBS (pH 7.0), and DPV scans were obtained. They showed strong anodic peaks at about −0.27 V *versus* SCE (a in Fig 4A; State I in Scheme 2). This modified electrode was immersed in PBS for 4 h with stirring. Under these conditions, it was expected that some of the loaded MB immobilized by non-specific binding, would be released from the film, and the DPV profiles would decrease significantly as, indeed, is illustrated in b, Fig 4A, and State II, Scheme 2. Subsequently, the electrode in its treated or modified state, as the case may be, was re-immersed into the MB solution for 2 h to facilitate the reloading of the MB. The MB-dsDNA/GO-CS/AuNPs/GCE produced very similar DPV profiles (a and c, Fig 4A). This indicated that the loading/releasing of MB was readily reversible and the dsDNA/GO-CS/AuNPs film on the electrode was quite stable and able to retain its original structure and binding capability.

The ability of the MB molecule to be stabilised and retained well inside of the dsDNA/GO-CS/AuNPs film was also investigated. This was achieved by comparing the influence of the immersion time of the treated electrode in PBS on the DPV oxidation peak current (I_{pa}) after MB was loaded on the film for 2 h. This experiment showed that the MB was gradually released from the film into the buffer (Fig. 4B), and when compared with the initial peak current, it was evident that about 65% of MB was retained in the film after immersion for 30 min. Even after further immersion of up to 6 h in the PBS, about 30% of the initial DPV peak current was still recorded; thereafter, the DPV peak current decreased slowly.

3.4. Detection of natural DNA damage induced by BPA, NP or OP

The DPVs (Fig. 5) were collected with the use of the MB-dsDNA/GO-CS/AuNPs/GCE, which was immersed in a PBS (pH 7.0); this contained sufficient amount of BPA, NP or OP solute so as to produce

solutions of the same concentration. The electrode was immersed for different periods of time. The anodic peak currents decreased with the increase in the immersion time. This indicated that the DNA films damaged by BPA, NP or OP cannot reload as much MB as with the undamaged DNA films, and thus, this observation suggested that the interaction between EDCs and dsDNA was irreversible, i.e. DNA damage could be induced by the EDCs.

In order to investigate the extent of the damage to the DNA films induced by BPA, NP or OP, the damage rate of the DNA in a film deposited on the electrode, was estimated from the slope of the linear plot of the peak current ratio ($I_{P,I}$ / $I_{P,IV}$) *versus* treatment time with BPA, NP or OP (inset, Fig. 5), where $I_{P,I}$ and $I_{P,VI}$ were the DPV peak currents of the MB-dsDNA/GO-CS/AuNPs films in States I and IV (Scheme 2), respectively. In these experiments, each electrode was used only once during the reaction process from State I to State III. In order to correct for any electrode−to−electrode variations, the relative peak current ratio ($I_{P,I}$ / $I_{P,IV}$) was used for any calculations, instead of the absolute peak current, ($I_{P,IV}$). This ratio, ($I_{P,I}$ / $I_{P,IV}$), increased linearly with the BPA, NP or OP preparation time from 20 to 120 min, and over 120 min, the decrease of $I_{P,IV}$ was not significant, i.e. the amount of DNA damage was approaching stability. The related damage rates were 0.0069, 0.0044 and 0.0031 min^{-1}, with correlation coefficients of 0.995, 0.986 and 0.997, respectively. This indicated that the reaction between BPA and DNA produced most severe damage; the damage was less severe during the reaction between OP and DNA under the same conditions.

3.5. Detection of DNA damage by the EIS technique

The EIS technique is well−known for the detection of DNA damage [17], and in this work, it was use to verify any damage induced by BPA, NP or OP; it was shown that the DNA/GO-CS/AuNPs/GCE displayed relatively high charge transfer resistance (see arrow on curve a, Fig. 6), which occurred because the electronegative phosphate backbone of the DNA prevented the $[Fe(CN)_6]^{3-/4-}$ from reaching the surface of the electrode [40]. Subsequently, DNA/GO-CS/AuNPs/GCE was treated in 1.0×10^{-5} mol L^{-1} BPA, NP or OP solution for 30 min at 37 °C, respectively, and a slight increase in charge transfer resistance value was detected, i.e. the semicircle diameter was somewhat larger (see arrow, curve b, c and d, Fig. 6); this possibly occurred because the insertion of EDC molecules into the dsDNA reduces its charge transport. The insertion of the EDC molecules may result in a more negative charge environment on the dsDNA surface, which hinders accessibility of the $[Fe(CN)_6]^{3-/4-}$ anion. This may form a steric barrier at the base of the dsDNA

structure, which decreases the charge transport contribution of the dsDNA [20].

3.6. Interaction of DNA with BPA, NP or OP: DPSV analysis

Differential pulse stripping voltammetry (DPSV) was used to study the electrochemical behavior of BPA, NP or OP in the absence or presence of DNA at a GCE. The first profile (curve 1, Fig. 7) indicated that the anodic peaks for BPA, NP or OP, in the absence of DNA, occurred at 0.496, 0.540 and 0.504 V, respectively. When DNA was added to the BPA, NP or OP solutions (curves 2–9, Fig. 7), the compounds reacted with the DNA, respectively, and their associated peak currents clearly decreased. Also, the peak potentials shifted from 0.496, 0.540 and 0.504 V, respectively to the more positive values of 0.564, 0.632 and 0.620 V.

It has been noted [43] that the negative and positive peak potential shifts represented the electrostatic and hydrophobic interactions between the intercalated metal chelates and DNA, respectively. Thus, it is reasonable to suggest that the three EDCs, i.e. BPA, NP and OP, can interact with DNA to form a complex, primarily by intercalation, i.e. DNA−EDC_m, where 'm' is the stoichiometric coefficient. If this complex is stable, it is likely that some DNA may be damaged by this type of reaction at relatively high concentrations of the BPA, NP or OP compounds.

If it is assumed that the complex, DNA−EDC_m, was formed by EDC biding to DNA then:

$$DNA + mEDC \leftrightarrow DNA{-}EDC_m \quad (2)$$

where m is the stoichiometric binding coefficient, then the binding constant, K, can be evaluated from:

$$K = [DNA{-}EDC_m] / [DNA][EDC]^m \quad (3)$$

According to the Ilkovic equation for an irreversible electrode process [44]:

$$\Delta I_{max} = k\, c_{DNA} \quad (4)$$

$$\Delta I = k\, [DNA{-}EDC_m] \quad (5)$$

$$\Delta I_{max} - \Delta I = k(c_{DNA} - [DNA{-}EDC_m]); \text{ (note: } c_{DNA} = [DNA] + [DNA{-}EDA_m]) \quad (6)$$

On rearranging Eqs (3) – (6), the new expression is:

$$(1 / \Delta I) = (1 / \Delta I_{max}) + \{[1 / (K\Delta I_{max})] \times (1 / [EDC]^m)\} \quad (7)$$

or

$$\log [\Delta I /(\Delta I_{max} - \Delta I)] = m \log K + m \log[EDC] \quad (8)$$

where ΔI represents the difference in the oxidative current in the absence or presence of DNA, and the

maximum value of ΔI is $\Delta I_{max} c_{DNA}$. Also, [DNA] and [DNA−EDC_m] are the total, free and bound concentrations of DNA in the solution, respectively. If DNA interacts with EDC to form a single complex, then the plot of log [ΔI / (ΔI_{max} − ΔI)] *versus* log[EDC] should be linear with a slope, *m*, (Fig. 8), and the corresponding equations are:

$$\log[\Delta I / (\Delta I_{max} - \Delta I)] = 2.712 + 0.429 \log[BPA] \ (r = 0.9919) \quad (9)$$

$$\log[\Delta I / (\Delta I_{max} - \Delta I)] = 2.723 + 0.446 \log[NP] \ (r = 0.9931) \quad (10)$$

$$\log[\Delta I / (\Delta I_{max} - \Delta I)] = 2.552 + 0.427 \log[OP] \ (r = 0.9887) \quad (11)$$

According to the slope and intercept, the binding constants for BPA, NP and OP were calculated to be 2.09×10^6, 1.28×10^6 and $9.33 \times 10^5\ M^{-1}$. The results indicated that the interaction between BPA and DNA was the strongest, and that the interaction between OP and DNA system was the weakest under the same conditions. These findings are consistent with the conclusion in Section 3.4. A possible structure of the dsDNA-EDCs complex and the interaction caused by the addition of EDCs are shown in Scheme 1.

3.7. Reproducibility and stability of the sensor

The MB-dsDNA/GO-CS/AuNPs/GCE was prepared three times in PBS (pH 7.0) using the same GCE (pH 7.0) for DPV scans, and the average relative standard deviation (%RSD) of the peak current for MB was 7.23 ±0.68, which indicated that the modified electrode has acceptable reproducibility. Additionally, the stability of the modified electrode was estimated, and the sensor was immersed and stored in PBS (pH 7.0) for 15 days at 4 ºC. It was found that the anodic peak current of MB decreased by 18%. Thus, this result indicated that MB-dsDNA/GO-CS/AuNPs/GCE was reasonably stable.

4. Conclusions

The layer-by-layer construction method was used to construct a dsDNA/GO-CS/AuNPs, which were deposited on a GCE. This modified electrode was successfully used to detect indirectly DNA damage with the use of Methylene Blue (MB) acting as the electroactive probe. The damage was caused by any one of the three endocrine−disrupting compounds (EDCs) − bisphenol A (BPA), 4-nonylphenol (NP) and 4-t-octylphenol (OP). The results indicated that loading/releasing of MB at the dsDNA/GO-CS/AuNPs film is reversible. However, when the MB-dsDNA/GO-CS/AuNPs films were treated in BPA, NP or OP solution,

the peak current for MB ($I_{P,IV}$) significantly decreased in comparison to the $I_{P,I}$. This showed that the interaction between EDCs and dsDNA was irreversible, i.e. the DNA damage could be induced by EDCs. Also, the presence of any dsDNA damage was verified with the use of the EIS technique.

Acknowledgements

The authors gratefully acknowledge the financial support of this study by the National Natural Science Foundation of China (NSFC−31401587 and NSFC−21065007), the Natural Science Foundation of Jiangxi Province (20142BAB213009), and the State Key Laboratory of Food Science and Technology of Nanchang University (SKLF−ZZA201302 and SKLF−ZZB201303).

References

[1] P. Yakovchuk, E. Protozanova, M.D. Frank-Kamenetskii, Based-stacking and base-pairing contributions into thermal stability of the DNA double helix, Nucleic Acids Res. 34 (2006) 564−574.

[2] S. Gregory, K.F. Barlow, K.E. McLay, R. Kaul, D. Swarbreck, A. Dunham, C.E. Scott, K.L. Howe, K. Woodfine, The DNA sequence and biological annotation of human chromosome 1, Nature 441 (2006) 315−321.

[3] T. Ohta, S. Tokishita, K. Mochizuki, J. Kawase, M. Sakahira, H. Yamagata, UV sensitivity and mutagenesis of the extremely thermophilic eubacterium thermos thermophilus HB27, Genes Environ. 28 (2006) 56−61.

[4] J. Miyakoshi, M. Yoshida, K. Shibuya, M. Hiraoka, Exposure to strong magnetic fields at power frequency potentiates X−ray-induced DNA strand breaks, J. Radiat. Res. 41 (2000) 293−302.

[5] L. Hlavata, K. Benikova, V. Vyksocil, J. Labuda, Evaluation of damage to DNA induced by UV-C radiation and chemical agents using electrochemical biosensor based on low molecular weight DNA and screen−printed carbon electrode, Electrochim. Acta 71 (2012) 134−139.

[6] Worldometers−real time world statistics, http://www.worldometers.info/view/toxchem/, (accessed June 15, 2014)

[7] R. De Bont, N. Van Larebeke, Endogenous DNA damage in humans: a review of quantitative data, Mutagenesis 19 (2004) 169−185.

[8] D.K. La, J.A. Swenberg, DNA adducts: biological markers of exposure and potential applications to

risk assessment, Mutat. Res. 365 (1996) 129−146.

[9] F.P. Guengerich, Interactions of carcinogen-bound DNA with individual DNA polymerases, Chem. Rev. 106 (2006) 420−452.

[10] L.P. Zhou, J. Yang, C. Estavillo, J.D. Stuart, J.B. Schenkman, J.F. Rusling, Toxicity screening by electrochemical detection of DNA damage by metabolites generated in situ in ultrathin DNA−enzyme films, J. Am. Chem. Soc. 125 (2003) 1431−1436.

[11] Y. Liu, N.F. Hu, Loading/release behavior of (chitosan/DNA)n layer−by−layer films toward negatively charged anthraquinone and its application in electrochemical detection of natural DNA damage, Biosens. Bioelectron. 23 (2007) 661−667.

[12] Y.Y. Qiu, X.J. Qu, J. Dong, S.Y. Ai, R.X. Han, Electrochemical detection of DNA damage induced by acrylamide and its metabolite at the graphene-ionic liquid-nafion modified pyrolytic graphite electrode, J. Hazard. Mater. 190 (2011) 480−485.

[13] D.H. Atha, N. Ammanamanchi, M. Obadina, V. Reipa, Quantitative measurement of electrochemically induced DNA damage using capillary electrophoresis, J. Electrochem. Soc. 160 (2013) G3139−G3143.

[14] D. Anderson, J. Laubenthal, Analysis of DNA damage via single−cell electrophoresis, Methods Mol. Biol. 1054 (2013) 209−218.

[15] R.M. Vlad, M.C. Kolios, G.J. Gregory, Ultrasound imaging of apoptosis: spectroscopic detection of DNA-damage effects at high and low frequencies, DNA damage detection in situ, ex vivo, and in vivo: methods and protocols, Methods Mol. Biol. 682 (2011) 165−187.

[16] M. Frontini, M. Vijayakumar, A. Garvin, N. Clarke, A ChIP chip approach reveals a novel role for transcription factor IRF1 in the DNA damage response, Nucleic Acids Res. 37 (2009) 1073−1085.

[17] Y.N. Ni, P.P. Wang, H.Y. Song, X.Y. Lin, S. Kokot, Electrochemical detection of benzo(a)pyrene and related DNA damage using DNA/hemin/nafion-graphene biosensor, Anal. Chim. Acta 821 (2014) 34−40.

[18] T.L. Liao, Y.F. Wang, X.B. Zhou, Y. Zhang, X.H. Liu, J. Du, X.J. Li, X.Q. Lu, Detection of DNA damage induced by styrene oxide in dsDNA layer−by−layer films using adriamycin as electroactive probe, Colloids Surf. B 76 (2010) 334−339.

[19] S. Carlos, B. Oliveira, A.M. Oliveria−Brett, In situ DNA oxidative damage by electrochemically generated hydroxyl free radicals on a boron-doped diamond electrode, Langmuir 28 (2012)

4896−4901.

[20] L.P. Lu, L.H. Xu, T.F. Kang, S.Y. Cheng, Investigation of DNA damage treated with perfluorooctane sulfonate (PFOS) on ZrO_2 /DDAB active nano−order film, Biosens. Bioelectron. 35 (2012) 180−185.

[21] I. Lutz, W. Kloas, Amphibians as a model to study endocrine disruptors: I. Environmental pollution and estrogen receptor binding, Sci. Total Environ. 225 (1999) 49−57.

[22] J. Oehlmann, U. Schulte−Oehlmann, M. Tillmann, B. Markert, Effects of endocrine disruptors on prosobranch snails (Mollusca: Gastropoda) in the laboratory. Part I: Bisphenol A and octylphenol as xenoestrogens, Ecotoxicology 9 (2000) 383−397.

[23] P.H. Deng, Z.F. Xu, Y.F. Kuang, Electrochemical determination of bisphenol A in plastic bottled drinking water and canned beverages using a molecularly imprinted chitosan−graphene composite film modified electrode, Food Chem. 157 (2014) 490−497.

[24] Commission Directive 2011/8/EU of 28 January 2011, Amending Directive 2002/72/EC as regards the restriction of use of Bisphenol A in plastic infant feeding bottles.

[25] K.C. Chitra, C. Latchoumycandane, P.P. Mathur, Effect of nonylphenol on the antioxidant system in epididymal sperm of rats, Arch. Toxicol. 76 (2002) 545−551.

[26] G. Hernandez−Rodríguez, M. Zumbado, O.P. Luzardo, J.G. Monterde, A. Blanco, L.D. Boada, Multigenerational study of the hepatic effects exerted by the consumption of nonylphenol- and 4-octylphenol-contaminated drinking water in Sprague–Dawley rats, Environ. Toxicol. Pharmacol. 23 (2007) 73−81.

[27] C.G. Xie, H.F. Li, S.Q. Li, J. Wu, Z.P. Zhang, Surface molecular self-assembly for organophosphate pesticide imprinting in electropolymerized poly(p-aminothiophenol) membranes on a gold nanoparticle modified glassy carbon electrode, Anal. Chem. 82 (2010) 241−249.

[28] R.Z. Ouyang, S.A. Bragg, J.Q. Chambers, Z.L. Xue, Flower−like self−assembly of gold nanoparticles for highly sensitive electrochemical detection of chromium (VI), Anal. Chim. Acta 722 (2012) 1−7.

[29] K. Saha, S.S. Agasti, C. Kim, X.N. Li, V.M. Rotello, Gold nanoparticles in chemical and biological sensing, Chem. Rev. 112 (2012) 2739−2779.

[30] M.J. Allen, V.C. Tung, R.B. Kaner, Honeycomb carbon: a review of graphene, Chem. Rev. 110 (2010) 132−145.

[31] J.L. Chen, X.P. Yan, K. Meng, S.F. Wang, Graphene oxide based photoinduced charge transfer

label−free near−infrared fluorescent biosensor for dopamine, Anal. Chem. 83 (2011) 8787−8793.

[32] Y. Zhang, N.F. Hu, Cyclic voltammetric detection of chemical DNA damage induced by styrene oxide in natural dsDNA layer−by−layer films using methylene blue as electroactive probe, Electrochem. Commun. 9 (2007) 35−41.

[33] S.N. Sarma, Y.J. Kim, J.C. Ryu, Endocrine disrupting chemicals: 17 beta-estradiol, bisphenol A, nonylphenol and octylphenol induced DNA damage through the estrogen receptors-mediated regulation of H2AX, BRCA1 and MGP, Mol. Cell. Toxicol. 3 (2007) 54−54.

[34] Y.Y. Qiu, H. Fan, X. Liu, S.Y. Ai, T.T. Tang, R.X. Han, Electrochemical detect ion of DNA damage induced by in situ generated bisphenol A radicals through electro-oxidation, Microchim. Acta 171 (2010) 363−369.

[35] X.H. Jiang, W.J. Ding, C.L. Luan, Q.Q. Ma, Z.Y. Guo, Biosensor for bisphenol A leaching from baby bottles using a glassy carbon electrode modified with DNA and single walled carbon nanotubes, Microchim. Acta 180 (2013) 1021−1028.

[36] X.M. Meng, H.S. Yin, M.R. Xu, S.Y. Ai, J.Y. Zhu, Electrochemical determination of nonylphenol based on ionic liquid-functionalized graphene nanosh eet modified glassy carbon electrode and its interaction with DNA, J. Solid State Electrochem. 16 (2012) 2837−2843.

[37] X.Y. Lin, Y.N. Ni, S. Kokot, Glassy Glassy carbon electrodes modified with gold nanoparticles for the simultaneous determination of three food antioxidants, Anal. Chim. Acta 765 (2013) 54−62.

[38] Y.Y. Qiu, H. Fan, X. Liu, S.Y. Ai, T.T. Tang, R.X. Han, Electrochemical detection of DNA damage induced by in situ generated bisphenol A radicals through electro-oxidation, Microchim. Acta 171 (2010) 363−369.

[39] X.Y. Lin, Y.N. Ni, S. Kokot, A novel electrochemical sensor for the analysis of β−agonists: The poly(acid chrome blue K)/graphene oxide−nafion/glassy carbon electrode, J. Hazard. Mater. 260 (2013) 508−517.

[40] H. Dai, G.F. Xu, L.S. Gong, C.P. Yang, Y.Y. Lin, Y.J. Tong, J.H. Chen, G.N. Chen, Electrochemical detection of triclosan at a glassy carbon electrode modifies with carbon nanodots and chitosan, Electrochim. Acta 80 (2012) 362−367.

[41] H.Y. Song, Y.N. Ni, S. Kokot, Investigations of an electrochemical platform based on the layered MoS_2-graphene and horseradish peroxidase nanocomposite for direct electrochemistry and

electrocatalysis, Biosensors and Bioelectronics 56 (2014) 137−143.

[42] P.O. Vardevanyan, A.P. Antonyan, M.A. Parsadanyan, M.A. Shahinyan, L.A. Hambardzumyan, Mechanisms for binding between methylene blue and DNA, J. App. Spectros. 80 (2013) 595−599.

[43] Y.X. Wang, Y.N. Ni, S. Kokot, Voltammetric behavior of complexation of salbutamol with calf thymus DNA and its analytical application, Anal. Biochem. 419 (2011) 76−80.

[44] S.S. Kalanur, U. Katrahalli, J. Seetharamappa, Electrochemical studies and spectroscopic investigations on the interaction of an anticancer drug with DNA and their analytical applications, J. Electroanal. Chem. 636 (2009) 93−100.

Captions

Scheme 1. A stepwise, schematic representation of interactions of DNA with MB followed by the damaging effect of the EDC to form the DNA−EDC complex and related products. Structural formulae of three

endocrine - based disrupting compounds (EDCs) − bisphenol A (BPA), 4-nonylphenol (NP), 4-t-octylphenol (OP) as well as Methylene Blue (MB).

Scheme 2 A representation of the loading/release/reloading process of the MB in dsDNA/GO-CS/AuNPs films electro-deposited on a GCE. Corresponding DPV profiles are provided.

Fig. 1 SEM images: (**A**) GCE, (**B**) AuNPs/GCE and (**C**) GO-CS/AuNPs/GCE.

Fig. 2 Nyquist plots (**A**) and cyclic voltammograms (**B**) of: (**a**) GCE, (**b**) AuNPs/GCE, (**c**) GO-CS/AuNPs/GCE and (**d**) DNA/GO-CS/AuNPs/GCE. All electrodes were immersed in 0.1 mol L^{-1} KCl, which contained 5×10^{-3} mol L^{-1} $[Fe(CN)_6]^{3-/4-}$ (1:1); Nyquist plots were collected over the frequency range 0.01 - 1×10^{4} Hz, initial potential +0.256 V and amplitude 0.01 V; Chronocoulometric curves (**C**) were collected from: (**a**) GCE, (**b**) AuNPs/GCE, (**c**) CS/AuNPs/GCE and (**d**) GO−CS/AuNPs/GCE, for the reduction of 5×10^{-3} mol L^{-1} $K_3[Fe(CN)_6]$ in 0.1 mol L^{-1} KCl.

Fig. 3 DPV responses: (**a**) MB-DNA/GCE, (**b**) MB-DNA/AuNPs/GCE, (**c**) MB-DNA/CS/AuNPs/GCE, (**d**) MB-DNA/GO-CS/AuNPs/GCE and (**e**) MB/GO-CS/AuNPs/GCE in PBS (pH 7.0). The potential was scanned from - 0.6 to 0.1 V; amplitude: 0.05 V, pulse width: 0.06 s, and scan rate: 0.1 V s^{-1}.

Fig. 4 **(A)** DPV responses of MB-DNA/GO-CS/AuNPs/GCE immersed in PBS (pH 7.0): (**a**) in State I after the DNA/GO-CS/AuNPs/GCE was immersed in MB (1mmol L^{-1}) PBS (pH 7.0) for 2 h, (**b**) in State II after a 4 h immersion of the electrode in PBS (pH 7.0), and (**c**) after the electrode at State II was re−immersed in MB (1mmol L^{-1}) PBS (pH 7.0) for 2 h. Other conditions were as in Fig. 3. (**B**) Influence of the immersion time in the PBS (pH 7.0) on the DPV anodic peak current (I_{pa}) for the MB-DNA/GO-CS/AuNPs film deposited on a GCE (experiment repeated 3 times).

Fig. 5 DPV responses of MB-DNA/GO-CS/AuNPs/GCE immersed in PBS (pH 7.0), which produced State IV profiles for different treatment times. Experiments involved solutions containing 1.0×10^{-5} mol L^{-1} BPA, NP or OP compounds, which were kept at 37 °C and were stirred for 0−120 min. **Inset:** dependence of the peak current ratio, $I_{p,I}$ / $I_{p,IV}$, on treatment time of solutions containing BPA, NP or OP. The $I_{p,I}$ and $I_{p,IV}$ refer to the DPV anodic peak currents obtained from the above treated electrodes immersed in PBS (pH 7.0) and producing State I and State IV profiles, respectively. Other conditions were as in Fig. 3.

Fig. 6 Electrochemical impedance spectra (EIS) recorded in the 5×10^{-3} mol L^{-1} $[Fe(CN)_6]^{-3/-4}$ (1:1) solution with the use of: **(a)** DNA/GO-CS/AuNPs/GCE; immersed in 1.0×10^{-5} mol L^{-1} (**b**) BPA, (**c**) NP and

(**d**) OP solutions for 60 min at 37 °C, frequency range 0.01 - 1×10^4 Hz, initial potential +0.256 V and amplitude 0.01 V. Arrows represent the semicircle diameters.

Fig. 7 DPSV of 2.5×10^{-6} mol L^{-1} BPA, NP or OP in the absence (profile 1) and presence (profiles 2−9) of 5.0×10^{-7} ~ 4.0×10^{-6} mol L^{-1} DNA in PBS (pH 7.0) at a GCE. The potential was scanned from 0.2 to 1.0 V; scan rate : 100 mV s^{-1}, pulse width: 50 ms, pulse amplitude: 25 mV, and the deposition time: 60 s.

Fig. 8 Relationship between log [ΔI / (ΔI_{max} − ΔI)] and log [EDC] (log[BPA], log[NP] or log[OP]) at the MB-DNA/GO-CS/AuNPs/GCE in PBS (pH 7.0).

Scheme 1

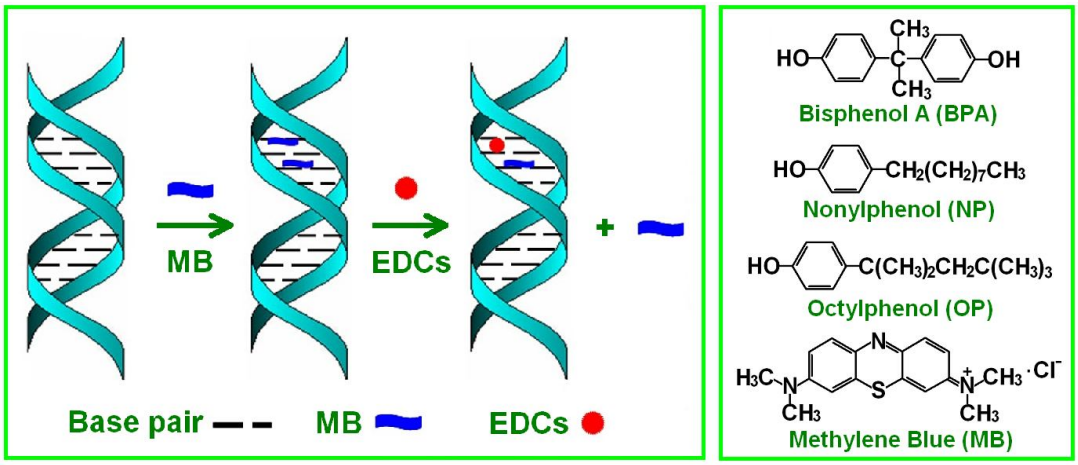

Scheme 2

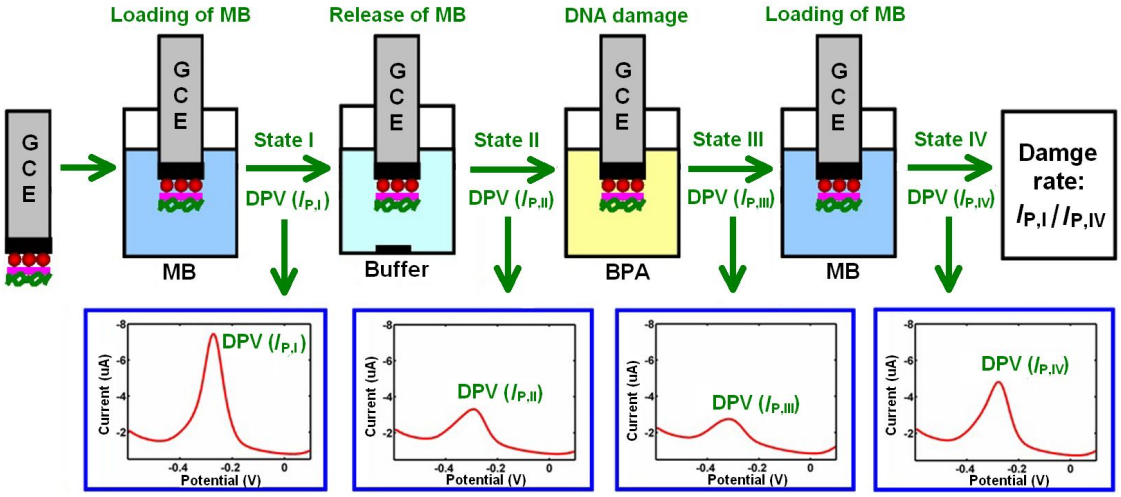

Fig. 1

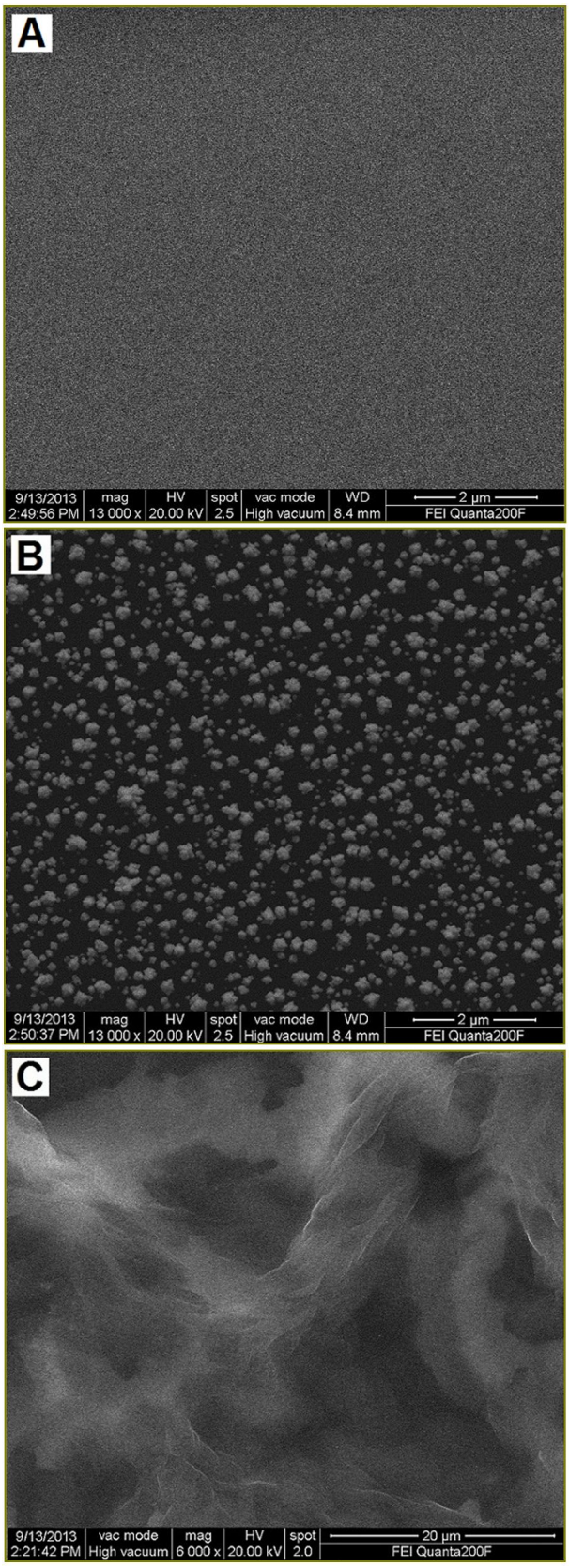

Fig. 2

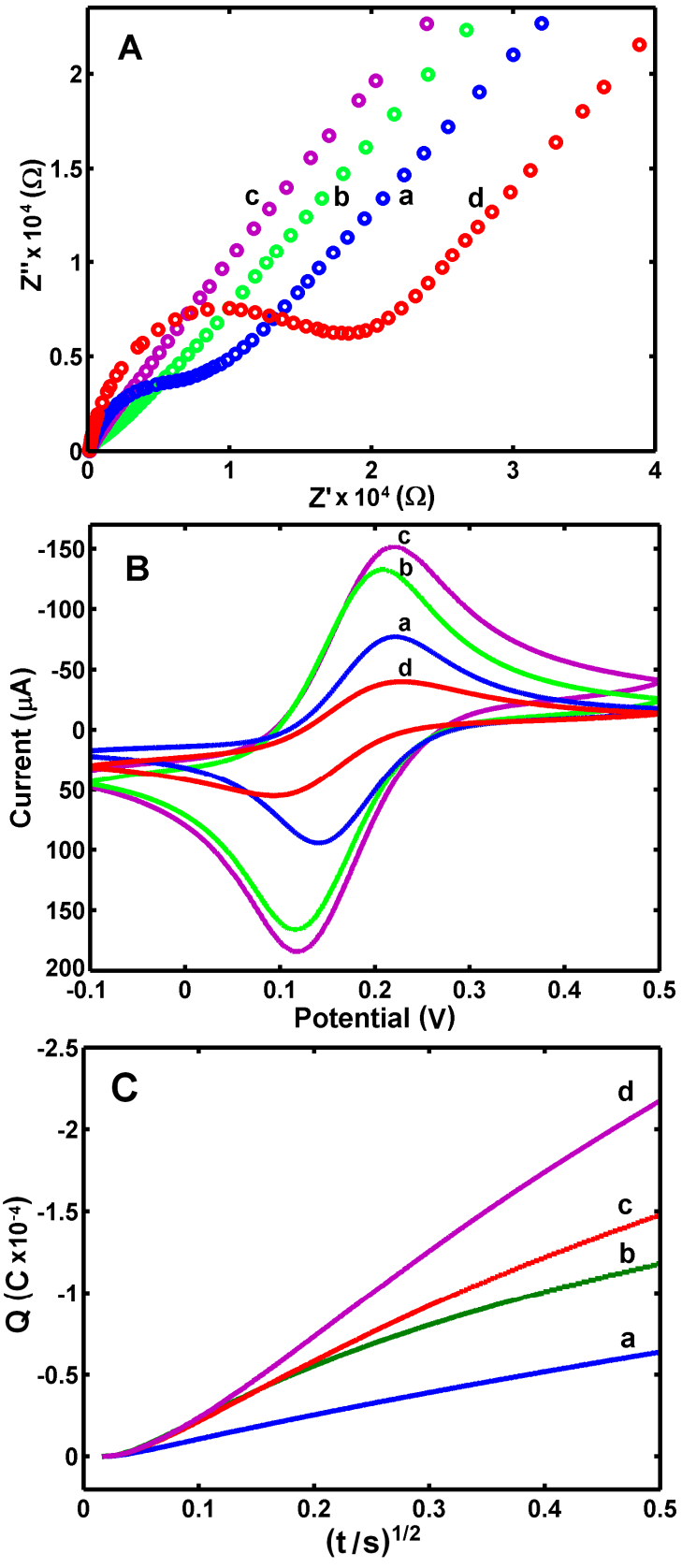

Fig. 3

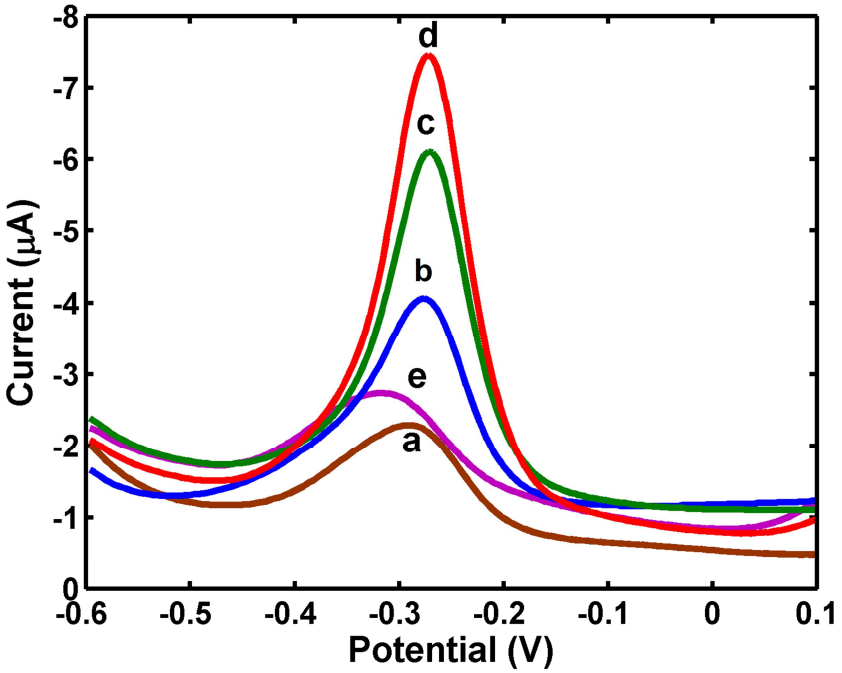

Fig. 4

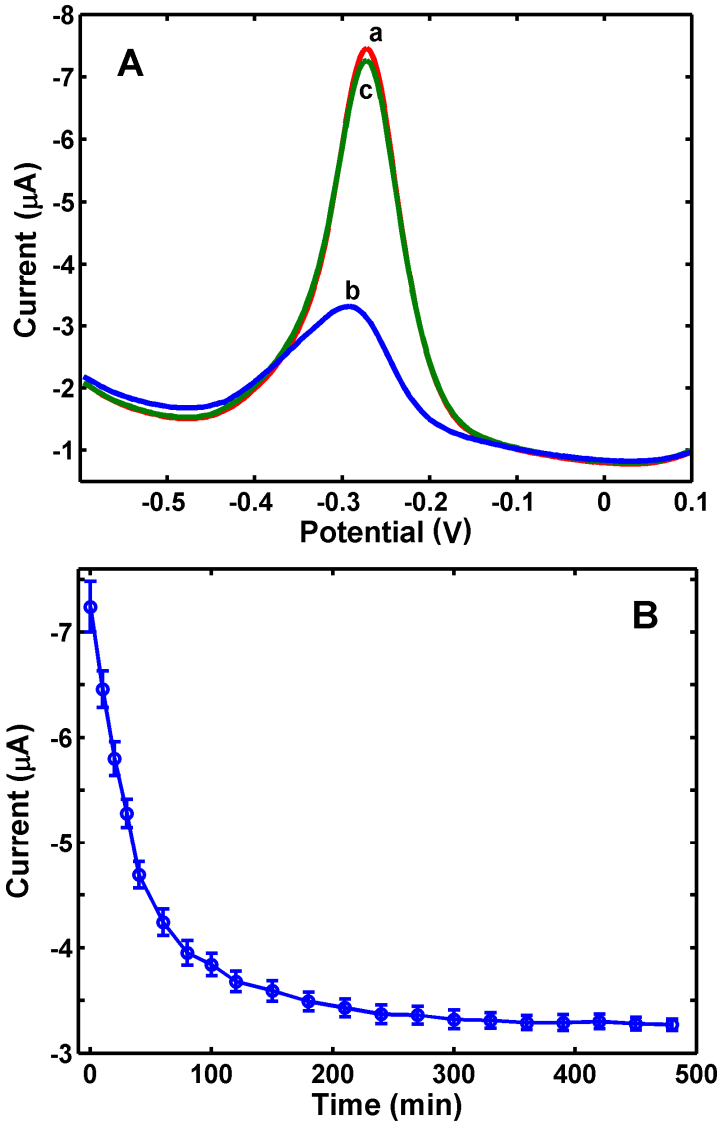

Fig. 5

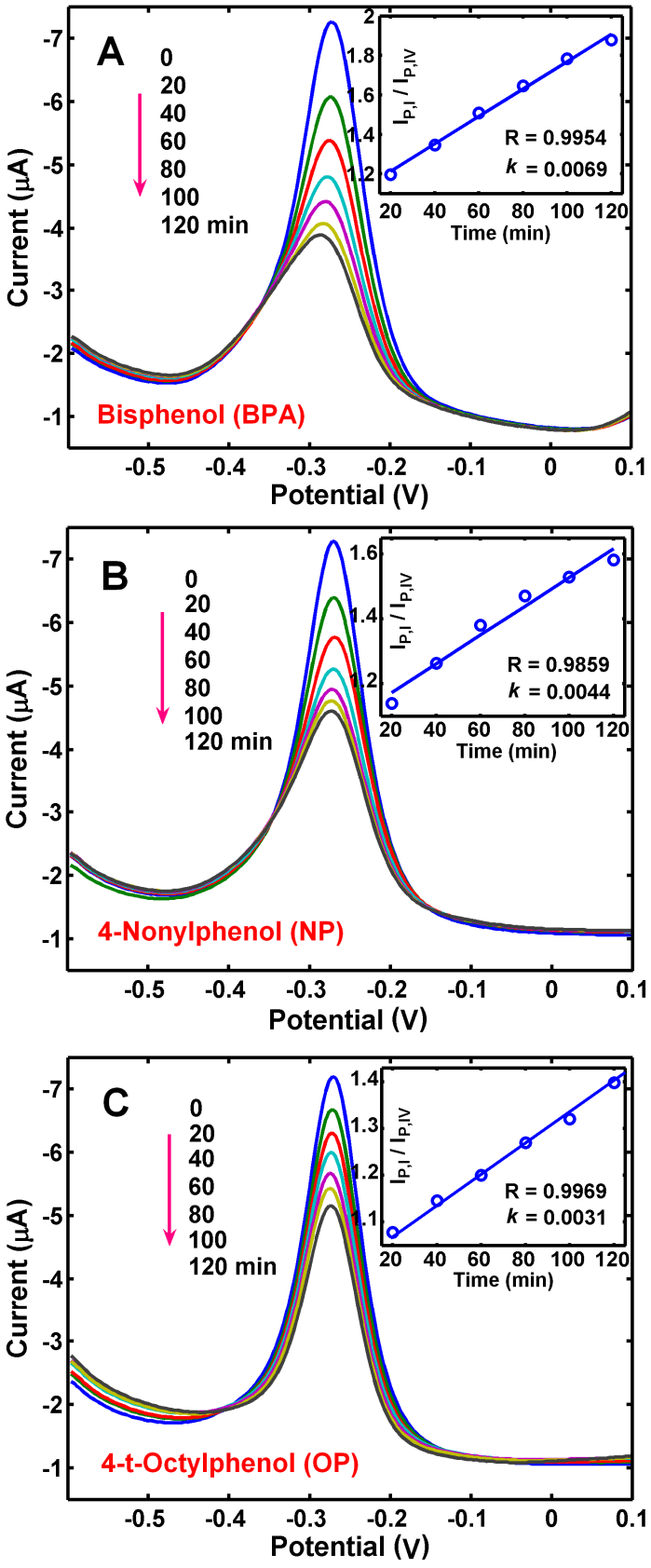

Fig. 6

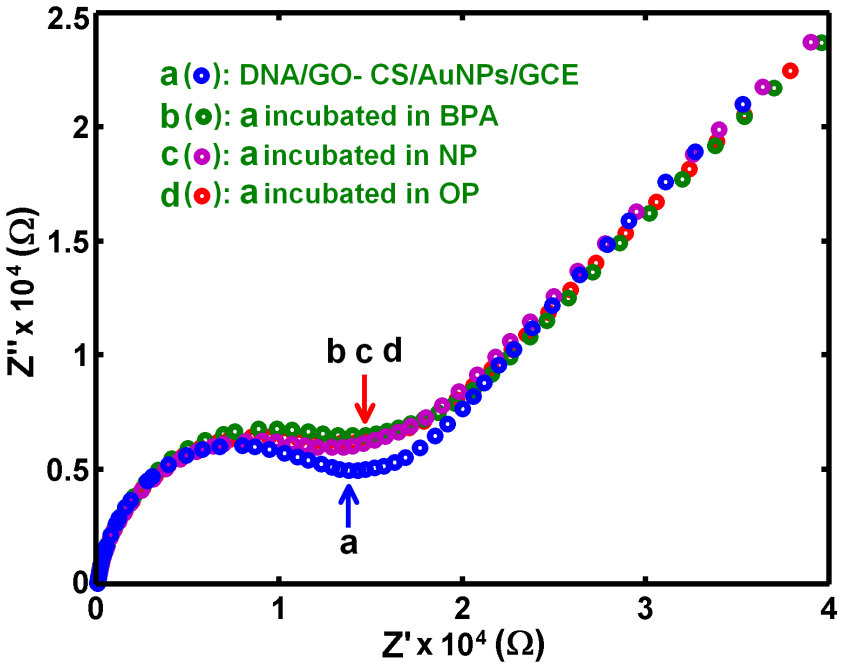

Fig. 7

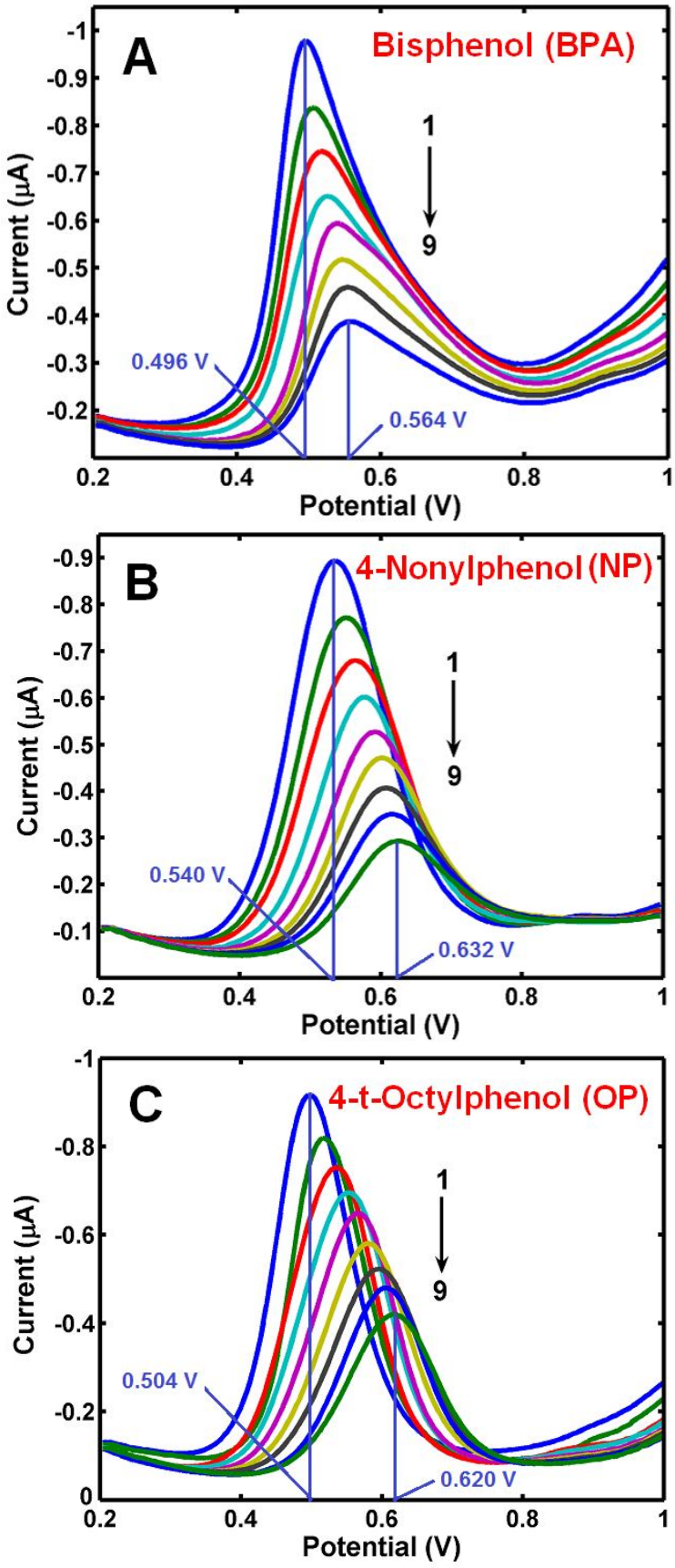

Fig. 8